

Photoemission Spectral Weight Transfer and Mass Renormalization in the Fermi-Liquid System $\text{La}_{1-x}\text{Sr}_x\text{TiO}_{3+y/2}$

T. Yoshida¹, A. Ino¹, T. Mizokawa², A. Fujimori^{1,2}, Y. Taguchi³, T. Katsufuji³, Y. Tokura³

¹*Department of Physics, University of Tokyo, Bunkyo-ku, Tokyo 113-0033, Japan*

²*Department of Complexity Science and Engineering, University of Tokyo, Bunkyo-ku, Tokyo 113-0033, Japan*

³*Department of Applied Physics, University of Tokyo, Bunkyo-ku, Tokyo 113-0033, Japan*

(September 2, 2018)

We have performed a photoemission study of $\text{La}_{1-x}\text{Sr}_x\text{TiO}_{3+y/2}$ near the filling-control metal-insulator transition (MIT) as a function of hole doping. Mass renormalization deduced from the spectral weight and the width of the quasi-particle band around the chemical potential μ is compared with that deduced from the electronic specific heat. The result implies that, near the MIT, band narrowing occurs strongly in the vicinity of μ . Spectral weight transfer occurs from the coherent to the incoherent parts upon antiferromagnetic ordering, which we associate with the partial gap opening at μ .

PACS numbers: 71.27.+a, 71.28.d, 79.60.Bm

The critical behavior of the electronic structure in the vicinity of the filling-control metal-insulator transition (MIT) has attracted much attention because of their fundamental importance [1] and their relevance to high- T_c superconductivity in layered cuprates. $\text{La}_{1-x}\text{Sr}_x\text{TiO}_3$ is a suitable system for investigating the filling-control MIT; their thermodynamic and transport properties have been systematically studied [2,3]. The system evolves from a Mott-Hubbard-type insulator having the d^1 configuration (LaTiO_3) to a band insulator having the d^0 configuration (SrTiO_3) with a wide range of the paramagnetic metallic (PM) phase in-between. Here, LaTiO_3 is antiferromagnetic below the Néel temperature $T_N \sim 140$ K [4]. Holes can be doped into LaTiO_3 by Sr substitution for La and/or by excess oxygens as in $\text{La}_{1-x}\text{Sr}_x\text{TiO}_{3+y/2}$ (LSTO), where $\delta = x + y$ is the hole concentration. The electrical resistivity ρ in the PM phase shows a T^2 dependence, characteristic of an interacting Fermi liquid [2,5]. With decreasing δ in the PM phase ($0.08 < \delta < 1$), the electronic specific heat coefficient γ , which is proportional to the conduction electron effective mass m^* , is enhanced towards the antiferromagnetic (AF) phase boundary ($\delta = 0.08$) and then decreases in the antiferromagnetic metallic (AFM) phase ($0.05 < \delta < 0.08$) and the antiferromagnetic insulating (AFI) phase ($\delta < 0.05$) [3,6]. The enhancement of γ is expected for correlated metals near a Mott transition, and has been analyzed within the Fermi-liquid framework [2,3].

Photoemission studies of the metallic bandwidth-control system $\text{Ca}_x\text{Sr}_{1-x}\text{VO}_3$ with the fixed band filling (d^1) [7] have indicated that the V 3d band is split into the quasi-particle band and the remnant of the Hubbard bands (the coherent and incoherent parts, respectively, of the spectral function) and that spectral weight transfer occurs between them as a function of U/W , where U is the one-site Coulomb repulsion and W is the one-electron band width, consistent with the prediction of dynamical mean-field theory (DMFT) [8]. However, the

effective mass obtained from the electronic specific heat coefficient γ and the magnetic susceptibility χ shows only a very weak enhancement with increasing U/W [9]. The Ti 3d band in the photoemission spectra of the filling-control systems LSTO [10] and $\text{Y}_{1-x}\text{Ca}_x\text{TiO}_3$ [11] also shows the same type of splitting into the coherent and incoherent parts, as has been predicted by DMFT [12]. In the present work, we have made a detailed photoemission study of LSTO ranging from the PM to AFM to AFI phases in order to clarify the electronic structure near the filling-control MIT. In particular, on the PM side of the PM-AFM phase transition, we discuss its effective mass renormalization based on the spectroscopic data and compare it with that deduced from the thermodynamic measurements. Since LSTO can be viewed as a normal Fermi liquid in the PM regime, it is interesting to compare its spectroscopic properties with those of the high- T_c cuprates, which show a remarkable deviation from the normal Fermi liquid in the underdoped regime. Therefore, we compare our results on LSTO with previous photoemission results on $\text{La}_{2-x}\text{Sr}_x\text{CuO}_4$ (LSCO) which show pseudogap behavior in the underdoped regime [13]. The filling-control MIT's in LSTO and LSCO may be considered as representative of the two types of Mott transitions caused, respectively, by a divergent effective mass m^* and a vanishing carrier number n [14].

Samples of $\text{La}_{1-x}\text{Sr}_x\text{TiO}_{3+y/2}$ and $\text{LaTiO}_{3+y/2}$ were melt grown by the floating-zone method in a reducing or inert atmosphere [15]. $\text{LaTiO}_{3+\delta/2}$ covers $\delta = 0.04, 0.06, \text{ and } 0.08$ and $\text{La}_{1-x}\text{Sr}_x\text{TiO}_{3+y/2}$ covers $\delta = 0.18, 0.28, 0.38, \text{ and } 0.65$. The δ values were determined by thermogravimetric analysis. Ultraviolet photoemission spectroscopy measurements were performed using a VSW hemispherical analyzer and a helium discharge lamp ($h\nu = 21.2$ eV). The total energy resolution was ~ 30 meV. The base pressure in the spectrometer was in the 10^{-10} Torr range. Clean surfaces were obtained by *in*

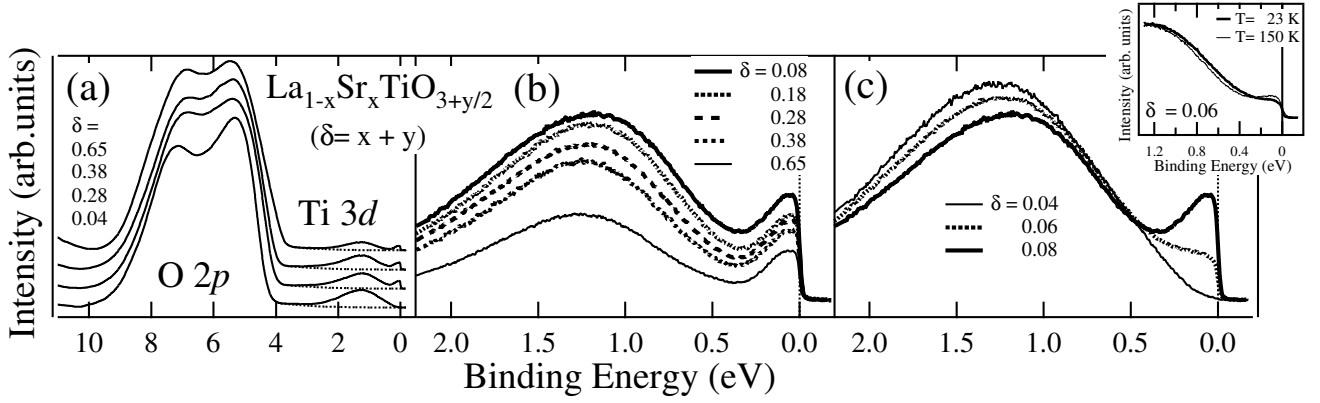


FIG. 1. Valence-band photoemission spectra of $\text{La}_{1-x}\text{Sr}_x\text{TiO}_{3+y/2}$ (a). The dotted curves are assumed backgrounds. Photoemission spectra of $\text{La}_{1-x}\text{Sr}_x\text{TiO}_{3+y/2}$ in the Ti 3d band region in the high doping regime (b) and the low doping regime (c). The inset shows the spectra of the AFM sample ($\delta=0.06$) below and above $T_N = 112$ K.

situ scraping with a diamond file. The electron chemical potential μ , namely, the Fermi level E_F was determined from the spectra of Au evaporated on each sample. The measurements were made at 20 K unless otherwise stated.

The valence-band photoemission spectra of LSTO show structures due to the O 2p and Ti 3d bands as shown in Fig. 1(a). In order to extract the Ti 3d band, we have assumed the tail of the O 2p band as shown by dotted curves in the figure. Figure 1(b)(c) shows the Ti 3d-band spectra thus deduced, whose integrated intensity has been normalized to the band filling $1 - \delta$. This normalization and the normalization to the integrated intensity of the O 2p band gave nearly identical results. The peak within ~ 0.3 eV of μ is the coherent part due to the quasi-particle excitation and corresponds to the renormalized Ti 3d band. The broad peak ~ 1.1 eV below μ is the incoherent part, reminiscent of the lower Hubbard band corresponding to the $d^1 \rightarrow d^0$ spectral weight of the insulating LaTiO_3 [8].

One can see that in going from $\delta = 0.65$ to 0.08 within the PM phase, both the coherent and incoherent parts become stronger [Fig. 1(b)], and in going from $\delta = 0.08$ to 0.06 in the AFM phase, the coherent part becomes weaker [Fig. 1(c)]. We consider that in the AFM phase a gap partially opens on the Fermi surface due to the AF ordering. As shown in the inset of Fig. 1(c), we observed for $\delta = 0.06$ that the spectral weight of the coherent part increases in going from below T_N ($= 112$ K) to above it. This fact implies that the suppression of the DOS of the coherent part is indeed due to the AF ordering and would be related to the increase of the resistivity of the $\delta = 0.06$ sample below ~ 100 K [6]. In the spectrum of the AFI ($\delta = 0.04$) sample, the spectral weight of the coherent part vanishes. Note that the spectral weight transfer from the coherent to the incoherent parts as shown in Fig. 1(c) involves energies as high as ~ 1 eV and cannot be explained by the ordinary spin-density-wave theory. Electron correlation effects would have to be invoked to

explain such behavior across the PM-AFM-AFI transitions.

In Fig. 2, the doping dependence of the spectral density of states (DOS) at μ , $\rho(\mu)$, is compared with the electronic specific heat coefficients γ and the Pauli paramagnetic susceptibility χ [2,3,6]. One can see from the figure that $\rho(\mu)$, γ , and χ show qualitatively similar doping dependencies; they increase with decreasing δ in the PM phase until the PM-AFM phase boundary ($\delta = 0.08$) is reached. However, a closer inspection reveals that while they all increase in the same way in the high doping regime ($\delta > 0.3$), γ and χ show faster increases than $\rho(\mu)$ in the low doping regime ($\delta < 0.3$) with decreasing δ .

In order to obtain further information about the mass renormalization of the conduction electrons in LSTO, we have evaluated the quasi-particle weight Z , the k -mass m_k , and the thermodynamic effective mass m^* [7,11,16] using the relationship $Z = \rho(\mu)/N^*(\mu)$, $m_k/m_b = \rho(\mu)/N_b(\mu)$, and $m^*/m_b = (1/Z)(m_k/m_b)$. Here, $N^*(\mu)$ is the density of quasi-particles deduced from $\gamma = (\pi^2/3k_B^2)N^*(\mu)$, m_b is the band mass, and $N_b(\mu)$ is the band DOS at μ derived from the PM band structure calculated using the local-density approximation (LDA) [17]. Z and m_k/m_b are given in terms of the self-energy $\Sigma(\mathbf{k}, \omega)$ by $Z = (1 - \partial \text{Re}\Sigma(\mathbf{k}, \omega)/\partial \omega|_{\omega=\mu, k=k_F})^{-1}$ and $m_k/m_b = (\partial \varepsilon_k/\partial k)/[\partial \varepsilon_k/\partial k + \partial \text{Re}\Sigma(\mathbf{k}, \omega)/\partial k]|_{\omega=\mu, k=k_F}$. Alternatively, we have evaluated Z by assuming that the spectral weight of the coherent part $S_{coh} \propto Z$ and that of the incoherent part $S_{incoh} \propto 1 - Z$, namely, by assuming that the mass renormalization is uniform throughout the quasi-particle band. Here, the Ti 3d band has been divided into the coherent and incoherent parts as shown in the inset of Fig. 3. We denote this Z by Z_S .

The doping dependence of Z and Z_S thus obtained is shown in Fig. 3(a). For $\delta > 0.2$, both Z and Z_S are small (~ 0.06), indicating strong correlation effects. Z further decreases with decreasing δ in the low doping regime

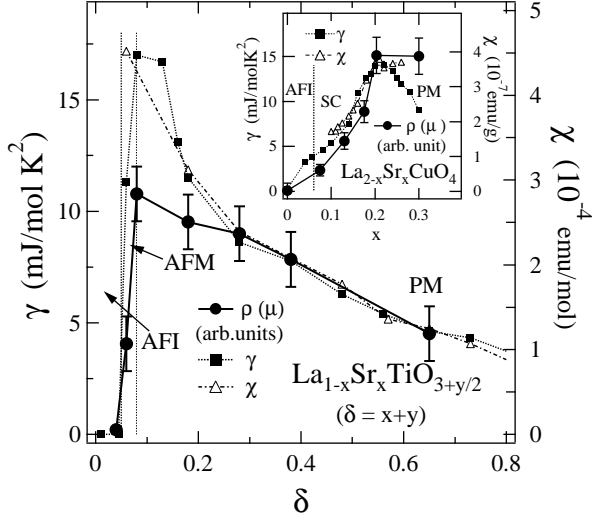


FIG. 2. Comparison of the DOS at μ , $\rho(\mu)$, with the electronic specific heat coefficient γ and the Pauli-paramagnetic susceptibility χ [2,3,6]. The inset shows $\rho(\mu)$, γ and χ of LSCO [13,20,21].

($\delta < 0.2$), indicating the increase of electron correlation effects. Since the decrease of Z is pronounced near the PM-AFM phase boundary, the effect of AF fluctuations may be responsible for it. On the other hand, Z_S does not decrease near the PM-AFM transition. The difference between Z and Z_S in the low doping regime means that the assumption of the uniform mass renormalization throughout the quasi-particle band breaks down in this δ regime. From this, we may conclude that band narrowing is particularly enhanced in the vicinity of μ near the PM-AFM boundary. Very recently, an angle-resolved photoemission study of Mo(110) surface states has shown that the band dispersion becomes less steep within ~ 50 meV of μ , indicating a strong energy dependence of $\partial \text{Re}\Sigma(\mathbf{k}, \omega)/\partial \omega$ in the vicinity of μ , which has been attributed to electron-phonon interaction [18]. In Fig. 3(b), the k -mass m_k/m_b shows a weak increase with decreasing δ in the PM phase. This is contrasted with the bandwidth-control MIT in $\text{Ca}_{1-x}\text{Sr}_x\text{VO}_3$, where m_k rapidly decreases with increasing U/W [7].

We then evaluate the mass enhancement factor m^*/m_b from the spectroscopic data using the two methods: $m_S^*/m_b = (m_k/m_b)(1/Z_S)$ and $m_W^*/m_b = W_b/W_{coh}$ [7,11,16], where W_b is the bare band width from the LDA band-structure calculation [17] and W_{coh} is the quasi-particle band width observed by the photoemission experiment (see the inset of Fig 3). In Fig. 3(c), the doping dependence of m_S^*/m_b and m_W^*/m_b are compared with the thermodynamic effective mass $m^*/m_b = N^*(\mu)/N_b(\mu)$ deduced from γ . The doping dependence of m^*/m_b is weak in the high doping regime ($\delta > 0.3$) while it becomes stronger in the low doping regime ($\delta < 0.3$). In the high doping regime, where $Z_S \simeq Z$, both m_S^*/m_b

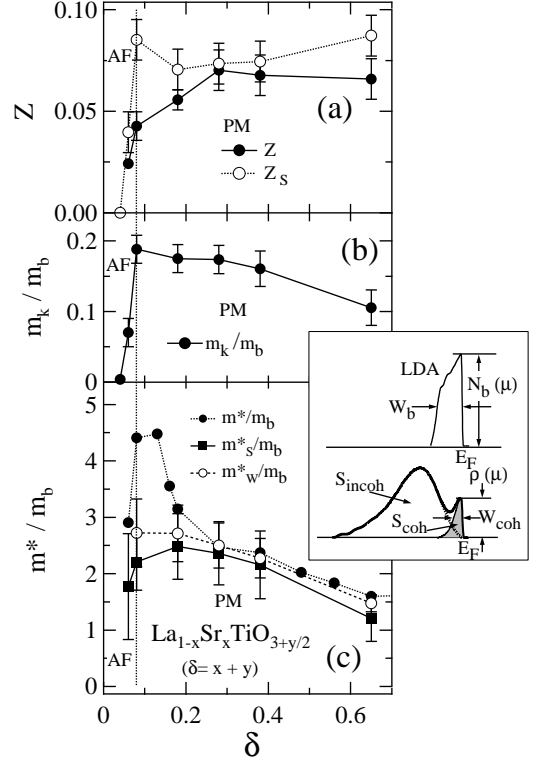


FIG. 3. Renormalization factor Z (a), the k -mass m_k (b), and the thermodynamic effective mass m^* (c) derived from various experiments. The inset shows how the lineshape of the Ti 3d band has been analyzed when deriving $m_S^*/m_b = (m_k/m_b)(1/Z_S) = (N_b(\mu)/\rho(\mu))(1 + S_{incoh}/S_{coh})$ and $m_W^*/m_b = (W_b/W_{coh})$.

and m_W^*/m_b agree with m^*/m_b , indicating that the quasi-particle band is uniformly narrowed. Near the PM-AFM phase boundary, on the other hand, m_S^*/m_b and m_W^*/m_b are not so enhanced as m^*/m_b . This again indicates that the band narrowing does not occur uniformly by the factor m_S^*/m_b or m_W^*/m_b in the quasi-particle band, but more strongly in the vicinity of μ .

While the overall behavior of the spectral lineshapes and the spectroscopic and thermodynamic mass renormalization in LSTO is consistent with the prediction of DMFT [12], some discrepancies are noted: DMFT predicts a rather uniform band narrowing and a constant $m_k/m_b (= 1)$, leading to $Z \simeq Z_S$ and $m^* \simeq m_S^* \simeq m_W^*$ in the entire doping range. The discrepancies between m^* , m_S^* and m_W^* described above, particularly in the low doping regime, indicate that AF fluctuations, which are not included in DMFT, may play some role near the MIT.

Now, we consider the effect of surface states on the above analyses for LSTO, because there is a possibility that the incoherent part includes contributions from the surface states as in the case of the perovskite-type $\text{La}_{1-x}\text{Ca}_x\text{VO}_3$ (LCVO) [19]. Surface contributions in

LSTO should be smaller than in LCVO, because the O 1s core-level spectra of LSTO show a single peak for all the samples, in contrast to LCVO which shows multiple peak structures owing to possible charge disproportionation into V^{3+} and V^{5+} on the surface. Nevertheless, we have estimated to what extent the present analyses are altered if surface contributions exist. We assume that the surface-derived spectral weight in the Ti 3d band region is $\alpha S(\alpha < 1)$ compared to the bulk contribution $S \equiv S_{coh} + S_{incoh}$, and that the surface signals contribute only to the incoherent part as in the case of LCVO [19]. Under this assumption, $\rho(\mu)$ and S_{coh} should be multiplied by $1/(1 - \alpha)$ and hence Z , Z_S and m_k/m_b by $1/(1 - \alpha)$ as a correction for the surface contribution. Hence, the doping dependence of these quantities would not change although their absolute values are multiplied by $1/(1 - \alpha)$. Furthermore, $m_S^*/m_b = (m_k/m_b)(1/Z)$ would not change by this correction because the factor $1/(1 - \alpha)$ cancels out. m_W^*/m_b does not change, too, since it has been estimated by using only the band widths. Therefore we can say that if the surface contribution α is constant in the doping range considered here, the doping dependence of Z , Z_S , and m_k/m_b evaluated above remains valid, and the mass enhancement factor m_S^*/m_b or m_W^*/m_b remains unchanged after the correction.

It is interesting to compare the doping dependence of the mass renormalization in LSTO and that in LSCO in order to clarify what is common and what is different between the conventional Fermi liquid and the non-Fermi liquid of the underdoped cuprates. In the overdoped regime of LSCO, γ [20] and χ [21] increase with decreasing doping for $\delta > 0.2$, as shown in the inset of Fig. 2. This enhancement is similar to that in LSTO. However, for $0.1 < \delta < 0.2$, where LSCO is still in the PM (or superconducting) phase, γ , χ , and $\rho(\mu)$ decrease with decreasing δ because of the pseudogap opening [13]. Such pseudogap behavior has not been identified in the PM state of LSTO, although a very weak pseudogap has been postulated from magnetic susceptibility measurements at high temperatures (>300 K) [22]. The fact that the suppression of the density of quasi-particles in the PM phase of LSCO is comparable to that in the AFM state of LSTO may indicate that AF spin correlations in LSCO are strong enough to reduce the density of quasi-particles at μ . LSTO can therefore be considered as a normal Fermi liquid with negligible AF fluctuations except for near the PM-AFM phase boundary, while for $\delta < 0.08$ the static AF order suppresses the DOS as described above. In spite of the contrasting behavior of LSTO and LSCO, Z decreases with decreasing δ towards the PM-AFM phase boundary in both systems. It therefore appears that the decrease of Z , namely the loss of coherent spectral weight at and around μ , is a common feature of the two types of Mott transitions.

In conclusion, in the valence-band photoemission spectra of LSTO, the spectral DOS at μ , $\rho(\mu)$, is enhanced

towards the PM-AFM phase boundary in the PM phase, but is dramatically reduced in the AFM phase. In going from the PM to the AFM phases, spectral weight transfer takes place from the coherent part to the incoherent part. From the analyses of mass renormalization, it appears that near the PM-AFM transition, the band narrowing does not occur uniformly throughout the quasi-particle band, but preferentially in the vicinity of μ . The doping dependencies of $\rho(\mu)$, m^*/m_b , γ , and χ of LSTO are contrasted with those of LSCO. Although LSTO shows a systematic enhancement of quasi-particle density with decreasing δ in the PM phase, LSCO shows a suppression with decreasing δ in the PM (superconducting) phase at $\delta < 0.2$. These facts imply the importance of AF spin correlation in LSCO in this doping range.

We would like to thank Y. Takada and M. Imada for useful discussions and K. Kobayashi and T. Susaki for help in the measurements. This work is supported by a Special Coordination Fund from the Science and Technology Agency and the New Energy and Industrial Technology Development Organization (NEDO).

-
- [1] M. Imada, A. Fujimori, Y. Tokura, Rev. Mod. Phys. **70** 1039 (1998).
 - [2] Y. Tokura *et al.*, Phys. Rev. Lett. **70** 2126 (1992).
 - [3] K. Kumagai *et al.*, Phys. Rev. B **48** 7636 (1993).
 - [4] Y. Tokura, J. Phys. Chem. Solid. **53**, 1619 (1992).
 - [5] T. Katsufuji *et al.*, Phys. Rev. B **56** 10145 (1997).
 - [6] Y. Taguchi *et al.*, Phys. Rev. B **59** 7917 (1999).
 - [7] I. H. Inoue *et al.*, Phys. Rev. Lett. **74**, 2539 (1995).
 - [8] X. Y. Zhang, M. J. Rozenberg, and G. Kotliar, Phys. Rev. Lett. **70** 1666 (1992).
 - [9] I. H. Inoue *et al.*, Phys. Rev. B **58**, 4372 (1998).
 - [10] A. Fujimori *et al.*, Phys. Rev. B **46**, 9841 (1992).
 - [11] K. Morikawa *et al.*, Phys. Rev. B **54**, 8446 (1996).
 - [12] H. Kajueter, G. Kotliar, and G. Moeller, Phys. Rev. B **53** 16214 (1996).
 - [13] A. Ino *et al.*, Phys. Rev. Lett. **81** 2124 (1998).
 - [14] M. Imada, J. Phys. Soc. Jpn. **62**, 1105 (1993).
 - [15] Y. Fujishima, Y. Tokura, and T. Arima, Phys. Rev. B **46**, 11167 (1992).
 - [16] C. W. Greeff, H. R. Glyde, and B. E. Clements, Phys. Rev. B **45**, 7951 (1992).
 - [17] K. Takegahara, J. Electron Spectrosc. Related Phenom. **66**, 303 (1994).
 - [18] T. Valla *et al.*, Phys. Rev. Lett. **83**, 2085 (1999).
 - [19] K. Maiti, P. Mahadevan, and D. D. Sarma, Phys. Rev. Lett. **80**, 2885 (1998).
 - [20] N. Momono *et al.*, Physica C **233**, 395 (1994).
 - [21] T. Nakano *et al.*, Phys. Rev. B **49**, 16000 (1994).
 - [22] M. Onoda and M. Yasumoto, J. Phys. Cond. Matter. **9**, 3861 (1997); M. Onoda and M. Kohno, J. Phys. Cond. Matter. **10**, 1003 (1998).